Restoration of Normal L-Type Ca^{2+} Channel Function During Timothy Syndrome by Ablation of an Anchoring Protein

Edward P. Cheng, Can Yuan, Manuel F. Navedo, Rose E. Dixon, Madeline Nieves-Cintrón, John D. Scott, Luis F. Santana

Rationale: **L-type Ca^{2+} ($Ca_V1.2$) channels shape the cardiac action potential waveform and are essential for excitation–contraction coupling in heart. A gain-of-function G406R mutation in a cytoplasmic loop of $Ca_V1.2$ channels causes long QT syndrome 8 (LQT8), a disease also known as Timothy syndrome. However, the mechanisms by which this mutation enhances $Ca_V1.2$-LQT8 currents and generates lethal arrhythmias are unclear.**

Objective: **To test the hypothesis that the anchoring protein AKAP150 modulates $Ca_V1.2$-LQT8 channel gating in ventricular myocytes.**

Methods and Results: **Using a combination of molecular, imaging, and electrophysiological approaches, we discovered that $Ca_V1.2$-LQT8 channels are abnormally coupled to AKAP150. A pathophysiological consequence of forming this aberrant ion channel-anchoring protein complex is enhanced $Ca_V1.2$-LQT8 currents. This occurs through a mechanism whereby the anchoring protein functions like a subunit of $Ca_V1.2$-LQT8 channels that stabilizes the open conformation and augments the probability of coordinated openings of these channels. Ablation of AKAP150 restores normal gating in $Ca_V1.2$-LQT8 channels and protects the heart from arrhythmias.**

Conclusion: **We propose that AKAP150-dependent changes in $Ca_V1.2$-LQT8 channel gating may constitute a novel general mechanism for $Ca_V1.2$-driven arrhythmias. (*Circ Res*. 2011;109:255-261.)**

Key Words: $Ca_V1.2$ channels ■ EC coupling ■ calcium ■ arrhythmias

L-type Ca^{2+} ($Ca_V1.2$) channels are expressed in the sarcolemma of atrial and ventricular myocytes, where they play a critical role in activating Ca^{2+} release from the sarcoplasmic reticulum (SR) during excitation–contraction (EC) coupling. The magnitude and time course of the $Ca_V1.2$ current determine the waveform of the cardiac action potential (AP).[1] Thus, changes in $Ca_V1.2$ channel function can have profound effects on cardiac EC coupling and excitability. Accordingly, a recent study[2] discovered that a single amino acid substitution (G406R) in $Ca_V1.2$ is linked to Timothy syndrome. Timothy syndrome is characterized by prolongation of the electrocardiogram (ECG) QT interval and lethal arrhythmias, which is why it is also known as *long QT syndrome 8* (LQT8). Interest in the mechanisms of LQT8 has been intense because it is a multisystem disease, with many patients also afflicted by autism. Thus, a single amino acid mutation in $Ca_V1.2$ causes clinically significant disorders in the cardiac and central nervous systems.

Electrophysiological studies have revealed 2 distinctive features of LQT8 mutant $Ca_V1.2$ channels ($Ca_V1.2$-LQT8). First, these channels inactivate at a slower rate than do wild-type (WT) channels.[2–4] Second, small clusters of $Ca_V1.2$-LQT8 channels have a higher probability of undergoing coordinated openings and closings ("coupled gating") than do WT channels.[5] Although recent reports suggested that the G406R substitution in $Ca_V1.2$ creates a new phosphorylation site for the Ca^{2+}/calmodulin–dependent kinase II (CaMKII), which contributes to an increase in the open probability (P_o) of $Ca_V1.2$-LQT8 channels, others suggested that phosphorylation by CaMKII is not necessary for their slower rate of inactivation.[4,6,7] Thus, the mechanism by which the activity of $Ca_V1.2$-LQT8 channels is coordinated to generate irregular cardiac rhythm is unclear.

A potential mechanism regulating the activity of $Ca_V1.2$-LQT8 channels involves the anchoring protein AKAP150.

Original received May 10, 2011; revision received May 31, 2011; accepted June 13, 2011. In May 2011, the average time from submission to first decision for all original research papers submitted to *Circulation Research* was 14.5 days.

Brief UltraRapid Communications are designed to be a format for manuscripts that are of outstanding interest to the readership, report definitive observations, but have a relatively narrow scope. Less comprehensive than Regular Articles but still scientifically rigorous, BURCs present seminal findings that have the potential to open up new avenues of research. A decision on BURCs is rendered within 7 days of submission.

From the Department of Physiology & Biophysics, University of Washington, Seattle, WA (E.P.C., C.Y., M.F.N., R.E.D., M.N.-C., L.F.S.), and the Howard Hughes Medical Institute and Department of Pharmacology, University of Washington, Seattle, WA (J.D.S.).

Correspondence to Luis F. Santana, PhD, Department of Physiology & Biophysics, University of Washington, 1705 NE Pacific St HSB-G424, Box 357290, Seattle WA 98195. E-mail santana@uw.edu

Circulation Research **is available at http://circres.ahajournals.org** **DOI: 10.1161/CIRCRESAHA.111.248252**

Non-Standard Abbreviations and Acronyms	
AKAP150	A-kinase anchoring protein 150
AP	action potential
$[Ca^{2+}]_i$	intracellular Ca^{2+} concentration
CaM	calmodulin
CaMKII	Ca^{2+}/calmodulin-dependent kinase II
$Ca_V1.2$-LQT8	$Ca_V1.2$ channels with the long QT syndrome mutation
$Ca_V1.2$-WT	wild-type $Ca_V1.2$ channels
EC coupling	excitation–contraction coupling
ECG	electrocardiogram
LQT8	long QT syndrome 8 (Timothy syndrome)
LZ	leuzine zipper
MEF	mouse embryonic fibroblast
TdP	Torsades de pointes
tRFP	tag red fluorescent protein
WT	wild type

AKAP150 targets specific protein kinases and phosphatases to regions near $Ca_V1.2$ channels in ventricular myocytes and neurons.[8,9] Furthermore, AKAP150 binds to the carboxyl tail of $Ca_V1.2$ channels via leucine zipper (LZ) motifs in these 2 proteins,[10] facilitating physical interactions between $Ca_V1.2$ carboxyl tails. AKAP150 increases the probability of long openings and coupled gating events between $Ca_V1.2$ channels.[5] At present, however, whether the interaction with AKAP150 modulates the abnormal $Ca_V1.2$-LQT8 channel activity is unknown.

Here, we used a combination of cellular, molecular, imaging, and electrophysiological approaches to investigate this important issue. We discovered that AKAP150 is required for abnormal gating of $Ca_V1.2$-LQT8 channels. Importantly, our data indicate that ablation of AKAP150 corrects arrhythmogenic $Ca_V1.2$-LQT8 channel activity in ventricular myocytes.

Methods

An expanded Methods section is available in the Online Supplemental Material at http://circres.ahajournals.org.

Mice were euthanized using a lethal dose of sodium pentobarbital as approved by the University of Washington Institutional Animal Care and Use Committee. Details about the generation of our LQT8 mouse are available in the Online Supplemental Material. Ventricular myocytes were isolated as described previously.[8] Electrophysiological signals were recorded using HEKA EPC10 or Axopatch 200B amplifiers. Images were obtained using a confocal microscope. Data are presented as mean±SEM. A probability value of less than 0.05 was considered significant. An asterisk was used in the figure to illustrate a significant difference between groups.

Results

Ablation of AKAP150 Protects Against Cardiac Hypertrophy During LQT8

We generated a transgenic mouse that expresses $Ca_V1.2$-LQT8 channels fused to the tag-red fluorescent protein (tRFP) solely in cardiac myocytes (LQT8; Figure 1A) and crossed them with AKAP150 null mice (LQT8/AKAP150$^{-/-}$).[11] Online Table I summarizes 21 different anatomic and functional features of these mice. We found that the heart-to-body weight ratio of LQT8 hearts was larger than that of WT, AKAP150$^{-/-}$, and LQT8/AKAP150$^{-/-}$ mice. Indeed, LQT8 myocytes were longer and wider than WT, AKAP150$^{-/-}$, and LQT8/AKAP150$^{-/-}$ myocytes. These findings suggest that expression of $Ca_V1.2$-LQT8 promotes cardiac hypertrophy and loss of AKAP150 protects LQT8 mice against it.

AKAP150 Is Not Required for the Expression or Spatial Organization of $Ca_V1.2$-LQT8 Channels in Adult Ventricular Myocytes

Western blot analysis of biotinylated endogenous WT $Ca_V1.2$ ($Ca_V1.2$-WT) and $Ca_V1.2$-LQT8 indicated that sarcolemmal $Ca_V1.2$-WT expression was similar in WT, LQT8, AKAP150$^{-/-}$, and LQT8/AKAP150$^{-/-}$ myocytes (Figure 1B). $Ca_V1.2$-LQT8 channels comprised 41%±5 (n=6 mice) and 43%±4% (n=6 mice) of the total sarcolemmal $Ca_V1.2$ population in LQT8 and LQT8/AKAP150$^{-/-}$ myocytes, respectively. As with $Ca_V1.2$-WT channels in WT and AKAP150$^{-/-}$ myocytes, $Ca_V1.2$-LQT8 channels were prominently expressed along the transverse tubules (T-tubules) of LQT8 and LQT8/AKAP150$^{-/-}$ myocytes. However, unlike $Ca_V1.2$-WT channels, $Ca_V1.2$-LQT8 channels were also expressed in the intercalated discs and seemed to form multiple clusters in the sarcolemma and near the nuclear envelope of LQT8 and LQT8/AKAP150$^{-/-}$ cells (Figure 1C). The number of $Ca_V1.2$-LQT8 clusters were similar in LQT8 (Online Figure II, 154±7 clusters/cell, n=7) and LQT8/AKAP150$^{-/-}$ cells (142±68 clusters/cell, n=5; P>0.05) (see Online Supplemental material for a description of this analysis). Collectively, these data suggest that $Ca_V1.2$-LQT8 and CaV1.2-WT channels are differentially expressed in ventricular myocytes, but that AKAP150 does not regulate the expression or distribution of these channels in these myocytes.

Loss of AKAP150 Restores Normal Inactivation of I_{Ca} in LQT8 Myocytes

We recorded macroscopic $Ca_V1.2$ currents (I_{Ca}) from WT, AKAP150$^{-/-}$, LQT8, and LQT8/AKAP150$^{-/-}$ ventricular myocytes. Although the amplitude of I_{Ca} was similar in WT, AKAP150$^{-/-}$, LQT8, and LQT8/AKAP150$^{-/-}$ ventricular myocytes (P>0.05), there were striking differences in the rate of inactivation of these currents (Figure 2A and 2B and Online Table I). Indeed, the fraction of I_{Ca} remaining 50 ms (r_{50}) after the onset of depolarization to +10 mV from LQT8 myocytes was larger (n=8) than in WT (n=9) and AKAP150$^{-/-}$ myocytes (n=5; P<0.05), suggesting expression of functional $Ca_V1.2$-LQT8 channels in LQT8 myocytes. Indeed, from these I_{Ca} currents, we determined that $Ca_V1.2$-LQT8 channels account for ≈32% of the total $Ca_V1.2$ channel population in LQT8 myocytes (see Online Supplemental Material). Interestingly, the r_{50} of I_{Ca} in LQT8/AKAP150$^{-/-}$ (n=9) was similar to that of WT and AKAP150$^{-/-}$. These data suggest that loss of AKAP150 restores normal I_{Ca} inactivation in LQT8 myocytes.

Our I_{Ca} data raise an important question: is AKAP150 required for the expression of functional $Ca_V1.2$-LQT8 channels? To address this question, we expressed these channels

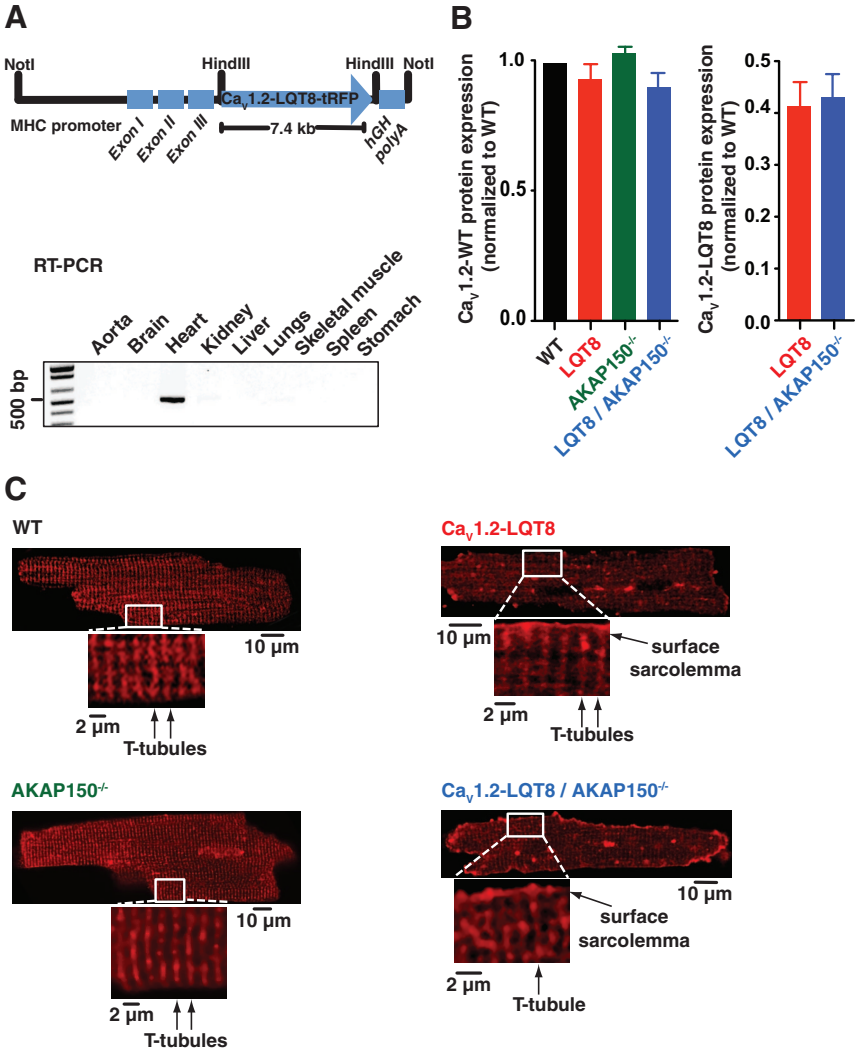

Figure 1. AKAP150 is not required for the expression and spatial distribution of $Ca_V1.2$-LQT8 channels in ventricular myocytes. A, Cardiac-specific expression of $Ca_V1.2$-LQT8 channels was achieved by using the α-myosin heavy chain (αMHC) promoter. The lower panel shows that expression of $Ca_V1.2$-LQT8 transcript was cardiac specific in LQT8 mice. **B**, Sarcolemmal wild-type (WT) and LQT8 $Ca_V1.2$ protein expression in WT, LQT8, AKAP150$^{-/-}$, and LQT8/AKAP150$^{-/-}$ myocytes. **C**, Confocal images of WT or LQT8 $Ca_V1.2$ channel-associated fluorescence in WT (immunofluorescence), LQT8 (tRFP fluorescence), AKAP150 (immunofluorescence), and LQT8/AKAP150$^{-/-}$ myocytes (tRFP fluorescence). Below each image, the section of the cell contained within the **white rectangles** is shown at higher magnification.

in WT and AKAP150$^{-/-}$ mouse embryonic fibroblasts (MEFs). As shown in Figure 2C, we recorded robust I_{Ca} (1 to 3 pA/pF) only in cells transfected with $Ca_V1.2$-WT or $Ca_V1.2$-LQT8. In WT MEFs (Figure 2C and 2D and Online Table I), $Ca_V1.2$-LQT8 currents (r_{50}=0.73±0.10, n=5) inactivated at a much slower rate than did $Ca_V1.2$-WT currents at +10 mV (r_{50}=0.25±0.02, n=6; P<0.05). However, in AKAP150$^{-/-}$ MEFs, $Ca_V1.2$-LQT8 channels (r_{50}=0.28±0.03, n=5) produced currents with a similar time course to that of $Ca_V1.2$-WT channels (r_{50}=0.35±0.03 at +10 mV; n=5 cells; P>0.05). Thus, although AKAP150 is not necessary for the expression of functional WT or LQT8 $Ca_V1.2$ channels, it is required for defective inactivation of $Ca_V1.2$-LQT8 channels.

A potential mechanism by which AKAP150 could promote a slow rate of inactivation of $Ca_V1.2$-LQT8 currents is by acting as an anchor for protein kinase A (PKA).[8,10] Another possibility is that the effects of AKAP150 on $Ca_V1.2$-LQT8 channel inactivation depend on CaMKII activity. Application of ht31 (PKA-AKAP interaction inhibitor, 10 μmol/L), Rp-cAMP (PKA inhibitor, 100 μmol/L), or KN-93 (CaMKII inhibitor, 5 μmol/L) did not change the r_{50} of I_{Ca} in LQT8 myocytes (Online Figure I, P>0.05), which suggests that PKA or CaMKII activity is not responsible for the potentiation of I_{Ca} during LQT8. Furthermore, these data support the view that the necessity of AKAP150 for decreased $Ca_V1.2$-LQT8 channel inactivation is not dependent on CaMKII activity or its ability to target PKA locally.

AKAP150 Is Required for Increased $Ca_V1.2$ Channel Activity and Coupled Gating Seen in LQT8 Myocytes

To test the hypothesis that ablation of AKAP150 decreases the P_o, open time, and frequency of coupled gating events by $Ca_V1.2$ channels in LQT8 myocytes, we recorded the in situ activity of $Ca_V1.2$ channels in WT, LQT8, and LQT8/AKAP150$^{-/-}$ myocytes using the cell-attached configuration of the patch clamp technique (Figure 3A and Online Table I). AKAP150$^{-/-}$ myocytes were not included in these experiments because the amplitude, rate of inactivation, and voltage dependence of I_{Ca} in these cells is similar to that of WT cells and LQT8/AKAP150$^{-/-}$ cells. Thus, it is unlikely that single $Ca_V1.2$ channel activity in AKAP150 null myocytes would be different from that of WT and LQT8/AKAP150$^{-/-}$ cells.

The amplitudes of elementary Ca^{2+} currents were similar in WT (0.55±0.10 pA, n=8 cells), LQT8 (0.60±0.11 pA,

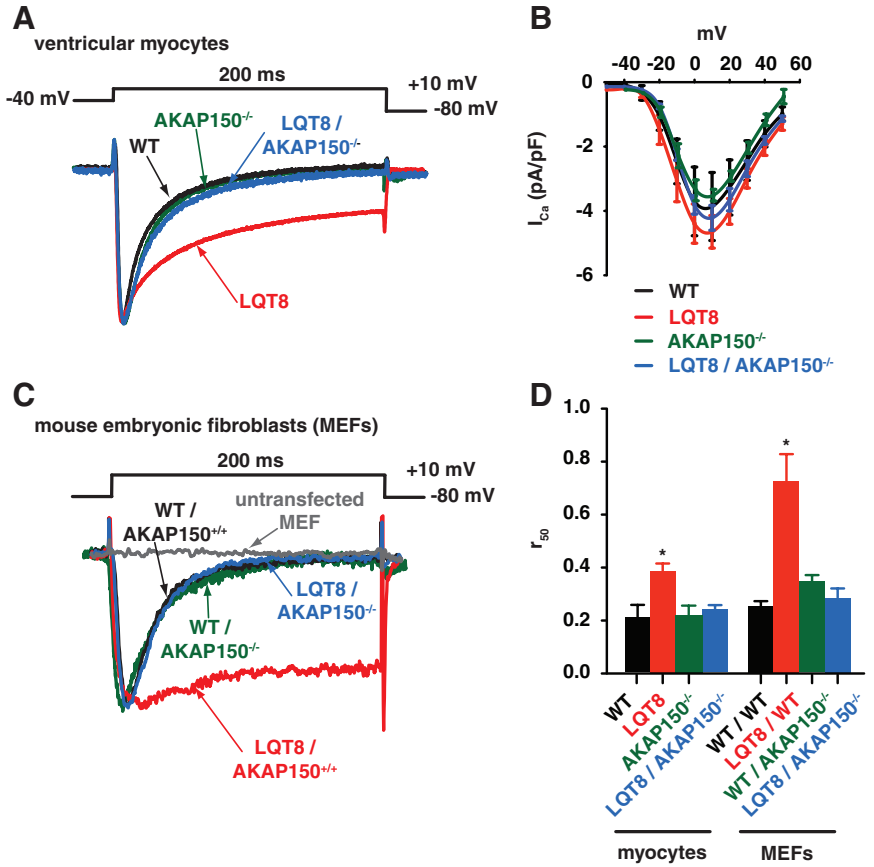

Figure 2. Loss of AKAP150 restores normal inactivation of I_{Ca} in LQT8 myocytes. A, Normalized I_{Ca} records from representative wild-type (WT), LQT8, AKAP150$^{-/-}$, and LQT8/AKAP150$^{-/-}$ ventricular myocytes. **B**, Current-voltage relationship of I_{Ca} in WT, LQT8, AKAP150$^{-/-}$, and LQT8/AKAP150$^{-/-}$ myocytes. **C**, I_{Ca} records from WT and AKAP150$^{-/-}$ mouse embryonic fibroblasts (MEFs) expressing either WT or LQT8 $Ca_V1.2$ channels. A current record from an untransfected MEF is also shown. **D**, Bar plot of the fraction r_{50} in ventricular myocytes or MEFs.

n=12 cells), and LQT8/AKAP150$^{-/-}$ (0.58±0.12 pA, n=10 cells) myocytes at −30 mV (P>0.05). Consistent with our I_{Ca} data, the activity (ie, NP_o where N is the number of channels and P_o is the open probability) of $Ca_V1.2$ channels in LQT8 myocytes (0.11±0.04) was ≈10-fold higher than in WT (0.01±0.01) and LQT8/AKAP150$^{-/-}$ (0.02±0.01) myocytes (P<0.05; Figure 3B). Furthermore, analysis of the open dwell times from $Ca_V1.2$ channels revealed that a larger proportion of channel openings are long openings in LQT8 myocytes in comparison with those recorded from LQT8/AKAP150$^{-/-}$ and WT myocytes. The open time histograms from WT and LQT8/AKAP150$^{-/-}$ myocytes could be fit with a single exponential function with a time constant (τ_{short}) of 0.8 ms and 0.6 ms, and the open time histogram of $Ca_V1.2$ channels in LQT8 myocytes could be fit with the sum of 2 exponential functions with τ_{short} of 1.3 ms and τ_{long} of 9.4 ms, which accounted for 95% and 5% of the channel openings, respectively (Figure 3B). The time constants from LQT8 myocytes likely represents a mixed population of WT and LQT8 $Ca_V1.2$ channels operating in 2 gating modalities in LQT8 myocytes. By contrast, the long $Ca_V1.2$ channel openings observed in LQT8 myocytes were completely absent in LQT8/AKAP150$^{-/-}$ cells. Collectively, these data suggest that AKAP150 is required for long openings of $Ca_V1.2$ channels in LQT8 myocytes.

To test the hypothesis that $Ca_V1.2$-LQT8 channels have a higher probability of coupled gating than do $Ca_V1.2$-WT channels in ventricular myocytes, we implemented a coupled Markov chain model to determine the coupling coefficient (κ) among $Ca_V1.2$ channels.[5,12] The mean coupling coefficient was 0.13±0.03 for Ca^{2+} channels in LQT8 myocytes and 0.03±0.01 for WT and 0.03±0.01 for LQT8/AKAP$^{-/-}$ cells (Figure 3D). Indeed, the frequency of coupled gating events (κ > 0.1) was higher in LQT8 (43%±10%) myocytes than in WT (8%±4%) and LQT8/AKAP150$^{-/-}$ (10%±6%) myocytes (P<0.05; Figure 3E).

Loss of AKAP150 Restores Normal $[Ca^{2+}]_i$, AP Waveform, and Cardiac Rhythm in LQT8 Mice

We recorded AP-evoked $[Ca^{2+}]_i$ transients in WT, LQT8, AKAP150$^{-/-}$, and LQT8/AKAP150$^{-/-}$ myocytes (Figure 4A and Online Table I). The amplitudes of the AP-evoked $[Ca^{2+}]_i$ transient in WT myocytes (n=7), AKAP150$^{-/-}$ (n=7), and LQT8/AKAP150$^{-/-}$ myocytes (n=9) were similar (P>0.05). The $[Ca^{2+}]_i$ transient was larger in LQT8 myocytes (n=9) than in these myocytes (P<0.05). Furthermore, although 56% of LQT8 myocytes had spontaneous Ca^{2+} release (SCR) events under control conditions, none was detected in WT, AKAP150$^{-/-}$, or LQT8/AKAP150$^{-/-}$ myocytes under similar experimental conditions. Because AKAP150 is required for β-adrenergic–induced increases in the amplitude of the AP-evoked $[Ca^{2+}]_i$ transient in ventricular myocytes,[8] we examined the effects of the β-adrenergic agonist isoproterenol (ISO, 100 nmol/L) on WT, LQT8, AKAP150$^{-/-}$, and LQT8/AKAP150$^{-/-}$ myocytes (Figure 4A and Online Table I). We found that ISO increased the amplitude of the AP-evoked $[Ca^{2+}]_i$ in WT and LQT8, but not in AKAP150$^{-/-}$ or LQT8/AKAP150$^{-/-}$ myocytes, pro-

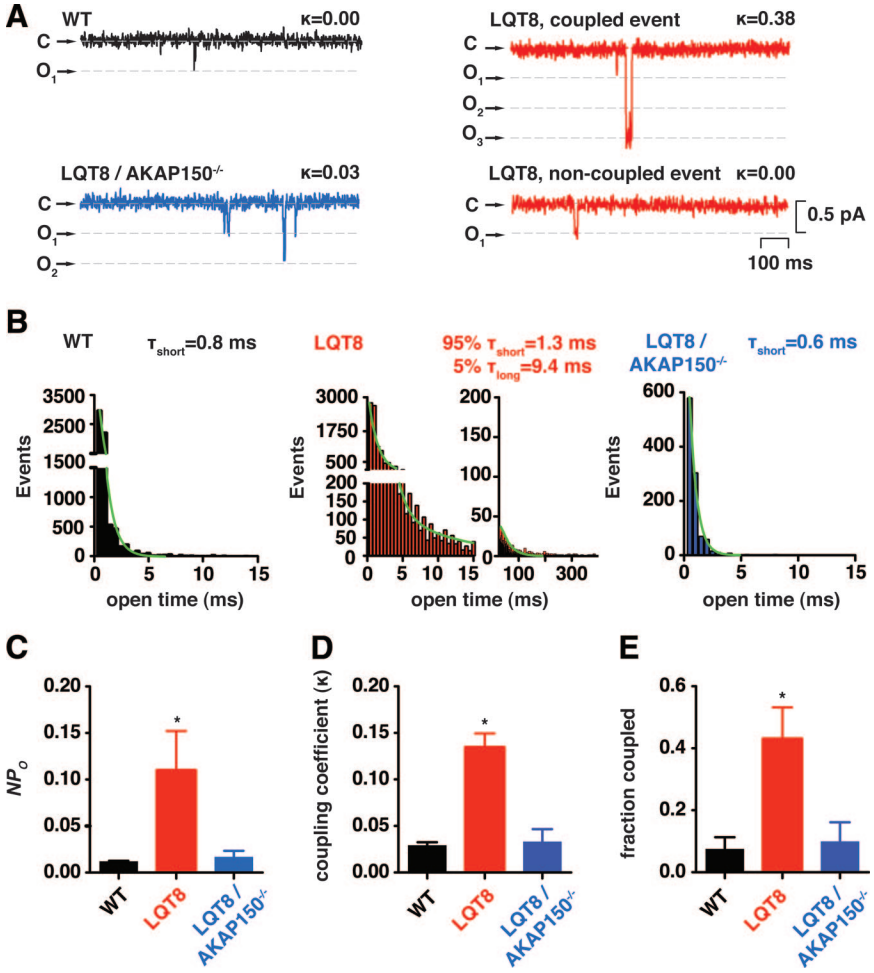

Figure 3. AKAP150 is required for increased in $Ca_V1.2$ channel activity and coupled gating seen in LQT8 myocytes. A, Exemplar cell-attached $Ca_V1.2$ channel currents from membrane patches recorded during a step depolarization to $^{-}30$ mV from $^{-}80$ mV, with various coupling coefficients (κ) from wild-type (WT), LQT8, and LQT8/AKAP150$^{-/-}$ ventricular myocytes. The 0 pA current level is marked by the letter *C*. **Dashed gray lines** show the amplitude of opening for 1 (O_1), 2 (O_2), or 3 (O_3) channels. **B**, Open dwell time histograms of $Ca_V1.2$ channel openings in WT (n=8 cells, 1 patch/cell), LQT8 (n=12 cells), and LQT8/AKAP150$^{-/-}$ (n=10 cells) myocytes. The time constants (τ) of exponential function fits (**green line**) of these histograms are shown. In LQT8 patches, a 2-term exponential fit with a τ_{short} and τ_{long} of 1.3 and 9.4 ms represent 95% and 5% of the entire population is optimal. Bar plots of the NP_O, κ, and the fraction of records with κ values >0.05 are shown in panels **C**, **D**, and **E**, respectively.

viding functional confirmation of the loss of AKAP150 in these cells (P<0.05). ISO also increased the number of spontaneous Ca^{2+} release events in $Ca_V1.2$-LQT8 cells from 40% to 85%, but not in WT, AKAP150$^{-/-}$, and LQT8/AKAP150$^{-/-}$ myocytes.

We investigated whether restoration of normal inactivation of I_{Ca} in LQT8/AKAP150$^{-/-}$ myocytes translated to changes in AP waveform in these cells. Consistent with our I_{Ca} data, the duration of the AP at 90% repolarization (APD_{90}) was longer in LQT8 (n=10) than in WT (n=5), AKAP150$^{-/-}$ (n=5), and LQT8/AKAP150$^{-/-}$ (n=11) myocytes (P<0.05; Figure 4B and Online Table I). In addition, analysis of records with trains of APs revealed that LQT8 myocytes had a higher frequency of early (EADs) and delayed afterdepolarizations (DADs) than did WT, AKAP150$^{-/-}$, and LQT8/AKAP150$^{-/-}$ myocytes (Figure 4C and Online Table I).

To determine the electrophysiological phenotype of WT, LQT8, AKAP150$^{-/-}$, and LQT8/AKAP150$^{-/-}$ mice, we implanted telemetric ECG transmitters[13] (Figure 4D and Online Table I). Heart rate was similar in WT (n=6), LQT8 (n=5), AKAP150$^{-/-}$ (n=6), and LQT8/AKAP150$^{-/-}$ at rest (n=6) or during mild exercise (P>0.05). However, consistent with our I_{Ca} and AP data, the QT interval—corrected for heart rate using Bazet's formula (ie, QT_c)—of LQT8 mice (116±1 ms) is longer than that of WT (97±1 ms), AKAP150$^{-/-}$ (98±1 ms), and LQT8/AKAP150$^{-/-}$ mice (108±1 ms; P<0.05). During exercise, although multiple premature ventricular depolarizations (PVDs) and episodes of *torsades de pointes* (TdPs, a hallmark of LQT) were observed in LQT8 mice, none was recorded from WT, AKAP150$^{-/-}$, and LQT8/AKAP150$^{-/-}$ mice (Figure 4D and Online Table I). Thus, loss of AKAP150 was protective against arrhythmias in mice expressing $Ca_V1.2$-LQT8.

Discussion

Our findings suggest a new model of $Ca_V1.2$-LQT8 channel dysfunction during Timothy syndrome (Figure 4E). In this model, the anchoring protein AKAP150 and $Ca_V1.2$-LQT8 form a complex that is necessary for aberrant $Ca_V1.2$-LQT8 channel gating and arrhythmias. $Ca_V1.2$-LQT8 channels likely interact with AKAP150 via LZ motifs in the carboxyl tails of both proteins.[10] We propose that AKAP150 functions like an allosteric modulator of $Ca_V1.2$-LQT8 channels, increasing $Ca_V1.2$-LQT8 currents by stabilizing the open conformation and increasing the probability of coupled gating between $Ca_V1.2$-LQT8 channels. This leads to increased Ca^{2+} influx, AP prolongation, cardiac hypertrophy, and arrhythmias. Coupled gating of $Ca_V1.2$-LQT8 channels presumably occurs because AKAP150 promotes physical interactions of adjacent channels via their carboxyl tails.[5,10,14]

Our data provide insights into the cellular mechanisms by which $Ca_V1.2$-LQT8 channels increase the probability of

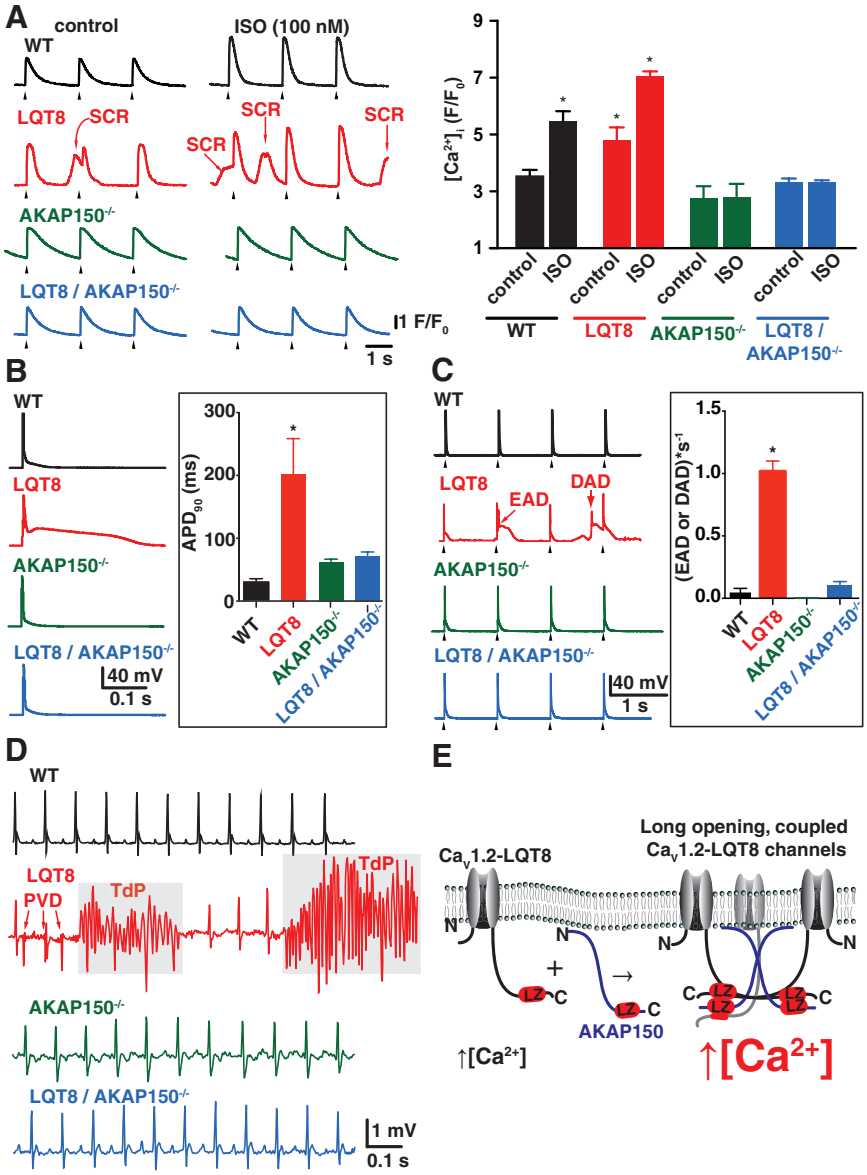

Figure 4. Loss of AKAP150 restores normal $[Ca^{2+}]_i$, AP waveform, and cardiac rhythm in LQT8 mice. A, $[Ca^{2+}]_i$ transients from representative wild-type (WT), LQT8, and LQT8/AKAP150$^{-/-}$ myocytes before and after the application of 100 nmol/L ISO. Spontaneous Ca^{2+} release events (SCR) in LQT8 myocytes are indicated. **Arrowheads** below indicate external stimuli. Bar plot represents the $[Ca^{2+}]_i$ transient amplitudes. **B**, APs from WT, LQT8, and LQT8/AKAP150$^{-/-}$ myocytes. (**Inset**) Bar plot of APD_{90}. **C**, Trains of APs recorded from WT, LQT8, AKAP150$^{-/-}$, and LQT8/AKAP150$^{-/-}$ myocytes. Early afterdepolarizations (EADs) and delayed afterdepolarizations (DADs) are indicated. **Arrowheads** below indicate current injection. The inset shows a bar plot of the rate of EADs or DADs in WT, LQT8, AKAP150$^{-/-}$, and LQT8/AKAP150$^{-/-}$ myocytes. **D**, ECG traces from WT, LQT8, and LQT8/AKAP150$^{-/-}$ mice. PVDs in the LQT8 trace are marked by **arrows**. The **gray** box highlights TdP in this LQT8 mouse. **E**, Proposed model of how AKAP150 binds to the C-terminal tail of $Ca_V1.2$-LQT8 channels, facilitating longer channel openings and interaction between multiple $Ca_V1.2$-LQT8 channels, which increases the frequency of coupled gating and greater Ca^{2+} influx, leading to arrhythmias.

arrhythmias. We found that expression of $Ca_V1.2$-LQT8 channels increased the frequency of arrhythmogenic EADs and DADs. EADs are likely produced by reactivation of $Ca_V1.2$ channels during the long APs of LQT8 myocytes. It is intriguing to speculate that the larger Ca^{2+} influx associated with $Ca_V1.2$-LQT8 channels leads to SR Ca^{2+} overload and thus to SRC events and DADs in LQT8 myocytes. Future experiments should examine in detail the relationship between Ca^{2+} influx via $Ca_V1.2$-LQT8 and EADs and DADs in these cells.

Ablation of AKAP150 corrects pathological $Ca_V1.2$-LQT8 channel gating and arrhythmias and prevents hypertrophy of LQT8 hearts presumably by decreasing Ca^{2+} influx via $Ca_V1.2$-LQT8 channels. Because AKAP150 does not bind CaMKII, loss of this scaffolding protein is not expected to affect CaMKII-dependent modulation of $Ca_V1.2$-LQT8 channels in ventricular myocytes. However, our data suggest that AKAP150 is required for any potential CaMKII-induced changes in $Ca_V1.2$-LQT8 gating. Thus, we propose that disrupting the interaction between AKAP150 and $Ca_V1.2$-LQT8 is a potential target for novel therapeutics for treating the broad spectrum of Timothy syndrome's symptoms, including lethal arrhythmias and autism.

Acknowledgments

We thank Dr Simon Hinke, Ms Jennifer Cabarrus and Katherine Forbush for technical assistance, Dr Richard D. Palmiter for helpful discussions, and Dr Michael T. Chin for reviewing ECG records.

Sources of Funding

Supported by the National Institutes of Health and the American Heart Association.

Disclosures

None.

References

1. Luo CH, Rudy Y. A model of the ventricular cardiac action potential. Depolarization, repolarization, and their interaction. *Circ Res*. 1991;68:1501–1526.

2. Splawski I, Timothy KW, Sharpe LM, Decher N, Kumar P, Bloise R, Napolitano C, Schwartz PJ, Joseph RM, Condouris K, Tager-Flusberg H, Priori SG, Sanguinetti MC, Keating MT. Ca(V)1.2 calcium channel dysfunction causes a multisystem disorder including arrhythmia and autism. *Cell*. 2004;119:19–31.
3. Barrett CF, Tsien RW. The Timothy syndrome mutation differentially affects voltage- and calcium-dependent inactivation of CaV1.2 L-type calcium channels. *Proc Natl Acad Sci U S A*. 2008;105:2157–2162.
4. Thiel WH, Chen B, Hund TJ, Koval OM, Purohit A, Song LS, Mohler PJ, Anderson ME. Proarrhythmic defects in Timothy syndrome require calmodulin kinase II. *Circulation*. 2008;118:2225–2234.
5. Navedo MF, Cheng EP, Yuan C, Votaw S, Molkentin JD, Scott JD, Santana LF. Increased coupled gating of L-type Ca^{2+} channels during hypertension and Timothy syndrome. *Circ Res*. 2010;106:748–756.
6. Erxleben C, Liao Y, Gentile S, Chin D, Gomez-Alegria C, Mori Y, Birnbaumer L, Armstrong DL. Cyclosporin and Timothy syndrome increase mode 2 gating of CaV1.2 calcium channels through aberrant phosphorylation of S6 helices. *Proc Natl Acad Sci U S A*. 2006;103:3932–3937.
7. Yarotskyy V, Gao G, Peterson BZ, Elmslie KS. The Timothy syndrome mutation of cardiac CaV1.2 (L-type) channels: multiple altered gating mechanisms and pharmacological restoration of inactivation. *J Physiol*. 2009;587:551–565.
8. Nichols CB, Rossow CF, Navedo MF, Westenbroek RE, Catterall WA, Santana LF, McKnight GS. Sympathetic stimulation of adult cardiomyocytes requires association of AKAP5 with a subpopulation of L-type calcium channels. *Circ Res*. 2010;107:747–756.
9. Coghlan VM, Perrino BA, Howard M, Langeberg LK, Hicks JB, Gallatin WM, Scott JD. Association of protein kinase A and protein phosphatase 2B with a common anchoring protein. *Science*. 1995;267:108–111.
10. Oliveria SF, Dell'Acqua ML, Sather WA. AKAP79/150 anchoring of calcineurin controls neuronal L-type Ca^{2+} channel activity and nuclear signaling. *Neuron*. 2007;55:261–275.
11. Tunquist BJ, Hoshi N, Guire ES, Zhang F, Mullendorff K, Langeberg LK, Raber J, Scott JD. Loss of AKAP150 perturbs distinct neuronal processes in mice. *Proc Natl Acad Sci U S A*. 2008;105:12557–12562.
12. Chung SH, Kennedy RA. Coupled Markov chain model: characterization of membrane channel currents with multiple conductance sublevels as partially coupled elementary pores. *Math Biosci*. 1996;133:111–137.
13. Mitchell GF, Jeron A, Koren G. Measurement of heart rate and Q-T interval in the conscious mouse. *Am J Physiol*. 1998;274:H747–H751.
14. Gold MG, Stengel F, Nygren PJ, Weisbrod CR, Bruce JE, Robinson CV, Barford D, Scott JD. Architecture and dynamics of an A-kinase anchoring protein 79 (AKAP79) signaling complex. *Proc Natl Acad Sci*. 2011;108:6426–6431.

Novelty and Significance

What Is Known?

- A single amino acid substitution in $Ca_V1.2$ L-type Ca^{2+} channels causes long QT syndrome 8 (LQT8).
- $Ca_V1.2$-LQT8 channels are characterized by an abnormally slow rate of inactivation and by exhibiting a high frequency of coordinated openings between nearby channels.
- The A-kinase anchoring protein 150 (AKAP150) is a $Ca_V1.2$ channel–associated scaffolding protein that regulates $Ca_V1.2$ channel function and excitation–contraction (EC) coupling by targeting adenyl cyclase 5, protein kinase A, and calcineurin near these channels.

What New Information Does This Article Contribute?

- AKAP150 is required for the expression of the LQT8 phenotype in a mouse model of this disease.
- AKAP150 functions like an allosteric modulator of $Ca_V1.2$-LQT8 channels that increases the opening time and also facilitates coupled gating between these channels in LQT8 cardiac myocytes.
- AKAP150 directly modulates the gating of $Ca_V1.2$-LQT8 without the aid of kinases.

The mechanism by which the LQT8 mutation alters the function of $Ca_V1.2$-LQT8 and EC coupling is unclear. Here, we establish that AKAP150 is necessary for the expression of the LQT8 phenotype. We find that AKAP150 functions as an accessory protein to the mutant $Ca_V1.2$-LQT8 channels, directly modulating the gating of these channels independently of its role in targeting adrenergic signaling. We also find that the coupled gating modality plays an important role in the pathophysiology of LQT8. The increased activity of $Ca_V1.2$-LQT8 in complex with AKAP150 increases the frequency of arrhythmogenic voltage fluctuations and arrhythmias. Our findings establish a novel role for AKAP150 as a $Ca_V1.2$ accessory protein in LQT8, and suggest that disruption of the interaction between $Ca_V1.2$ and AKAP150 could be a potential novel therapeutic target for LQT8 and other arrhythmias.

Cheng et al.

Supplement Material

Results

Phenotypic characteristics of LQT8 mice.

	WT	LQT8	AKAP150$^{-/-}$	LQT8/ AKAP150$^{-/-}$
Western blot				
% $Ca_V1.2$-LQT8	0	41 ± 5	0	43 ± 4
Whole –cell I_{Ca}				
r_{50} at +10 mV	0.21 ± 0.05	0.39 ± 0.03*	0.22 ± 0.03	0.24 ± 0.02
Maximum amplitude (pA/pF)	-3.98 ± 0.99	-5.12 ± 0.60	-3.59 ± 0.23	-4.27 ± 0.36
On-cell I_{Ca}				
NP_o	0.0121 ± 0.002	0.110 ± 0.042*	n.d.**	0.017 ± 0.007
Coupling coefficient (κ)	0.029 ± 0.005	0.134 ± 0.015*	n.d.	0.033 ± 0.013
Fraction coupled	0.08 ± 0.04	0.43 ± 0.10*	n.d.	0.10 ± 0.06
τ_{short} (ms)	0.8	1.3	n.d.	0.6
τ_{long} (ms)	-	9.4	n.d.	-
$[Ca^{2+}]_i$ transient				
Amplitude (F/F_0)	3.5 ± 0.2	4.8 ± 0.4*	2.5 ± 0.5	3.3 ± 0.1
Amplitude + 100 nM ISO (F/F_0)	5.5 ± 0.4*	7.1 ± 0.2*	2.7 ± 0.4	3.4 ± 0.1
AP				
APD_{90} (ms)	30 ± 5	253 ± 41*	56 ± 5	71 ± 6
(EAD or DAD) / s	0.06 ± 0.04	1.02 ± 0.08*	0	0.10 ± 0.03
ECG and arrhythmia				
Resting HR (beats/min)	694 ± 27	692 ± 23	677 ± 4	695 ± 18
Exercise HR (beats/min)	748 ± 3	757 ± 3	744 ± 4	755 ± 1
Arrhythmia frequency (% animals w/ tachyarrhythmia)	0	60%	0%	0%
QT_c Bazet (ms)	97 ± 1	116 ± 1*	105 ± 1	108 ± 1
Hypertrophy				
Heart weight/Body weight (mg/g)	4.75 ± 0.32	6.62 ± 0.65*	4.86 ± 0.36	5.07 ± 0.15
Cardiac myocyte length (μm)	107.2 ± 7.5	137.2 ± 8.9*	105.5 ± 4.3	103.2 ± 3.6
Cardiac myocyte width (μm)	25.8 ± 1.6	34.3 ± 2.0*	29.8 ± 5.5	24.6 ± 1.5
Contractility				
% Maximum fractional shortening	96 ± 2	91 ± 3	96 ± 2	96 ± 3
% Maximum fractional shortening + 100 nM ISO	89 ± 3	84 ± 3	97 ± 2*	95 ± 2

*p<0.05 **n.d.=not determined

Online Table I. Phenotypic characteristics of LQT8 mice.

Estimation of the relative number of $Ca_V1.2$-WT and $Ca_V1.2$-LQT8 channels in LQT8 myocytes

We determined the relative number of $Ca_V1.2$-WT and $Ca_V1.2$-LQT8 channels in LQT8 myocytes from macroscopic Ca^{2+} currents (I_{Ca}) in these cells as follows. Note that, in LQT8 myocytes, the macroscopic Ca^{2+} current is defined by the following equation:

$$I_{Ca} = I_{Ca,WT} + I_{Ca,LQT8}$$

where $I_{Ca,\,WT}$ and $I_{Ca,\,LQT8}$ are the currents produced by WT and LQT8 channels, respectively. At +10 mV, I_{Ca} records from WT myocytes suggest that $I_{Ca,WT}$ fully inactivates (i.e., $I_{Ca,\,WT}$ = 0 pA) at 200 ms. However, our data show that in LQT8 myocytes, I_{Ca} at 200 ms into a voltage step to +10 mV is ~1/3 that of the peak I_{Ca}. For a typical myocyte with a membrane capacitance of 100 pF, and assuming a peak current density of 3 pA/pF (recorded range 2.5-6.0 pA/pF) at +10 mV, the peak I_{Ca}=(100pF)(3 pA/PF)=300 pA. At 200 ms into a voltage step to +10 mV, I_{Ca}=(1/3)(300 pA)=100 pA. Thus, 200 ms into a voltage step to +10mV,

$$I_{Ca} = (NP_oR_{200}i_{Ca})_{LQT8} = 100\,pA$$

where N is the number of channels, P_o is the open probability, R_{200} is the fraction current remaining at 200 ms due to Ca^{2+} dependent inactivation only, and i_{Ca} is the unitary current of LQT8 channels. Our data suggest that WT and LQT8 channels have similar i_{Ca}. Although i_{Ca} in the presence of physiological 2 mmol/L Ca^{2+} at +10 mV is too small to measure, we used published values[1] and fit them with the Goldman, Hodgkin, and Katz (GHK) constant field equation. This gave a predicted i_{Ca} value of 0.05 pA at +10 mV. Assuming a maximum P_o value for $Ca_V1.2$-LQT8 channels of 0.5 and using the published value of 0.75 for R_{200} [2], then-

$$N_{LQT8} \approx \frac{100\,pA}{(0.5*0.7*0.05pA)} = 5714$$

Because at +10 mV, the P_o of $Ca_V1.2$-WT channels is 0.3 [3], we estimated the number of Cav1.2-WT channels at peak I_{Ca} as follows,

$$N_{WT} = \frac{I_{Ca} - (N_{LQT8}P_{o,LQT8}i_{Ca})}{(P_{o,WT}i_{Ca})} \approx \frac{300\,pA - \left(7143*0.5*0.05pA\right)}{0.3*0.05pA} = 12381$$

Thus, LQT8 channels account for ≈32% of the total number of channels in this exemplar LQT8 myocyte, a value that is in close agreement with our Western blot data (i.e., $Ca_V1.2$-LQT8 = 41 ± 5% of the total sarcolemmal $Ca_V1.2$ protein).

PKA or CaMKII do not modulate the rate of inactivation of I_{Ca} in LQT8 myocytes

We tested the hypothesis that AKAP150 modulates $Ca_V1.2$-LQT8 channel function independent of its ability to target PKA activity to specific regions of the ventricular myocyte. To do this, we recorded I_{Ca} in LQT8 myocytes before and after the application of 100 μM of the PKA inhibitor Rp-cAMP [4] or 10 μM of the PKA-AKAP interaction inhibitor Ht31 [5] (Online Figure I). Consistent

with our hypothesis, application of either Rp-cAMP or Ht31 did not change the r_{50} of I_{Ca} in LQT8 myocytes, suggesting that PKA is not responsible for the potentiation of I_{Ca} during LQT8. We also test the hypothesis that phosphorylation of $Ca_V1.2$-LQT8 by CaMKII causes delayed inactivation in these channels. Application of 5 μM of KN-93, a CaMKII inhibitor [6], did not restore r_{50} of I_{Ca} in LQT8 myocytes to WT levels, suggesting CaMKII activity is not required for slow I_{Ca} inactivation in these cells (Online Figure I).

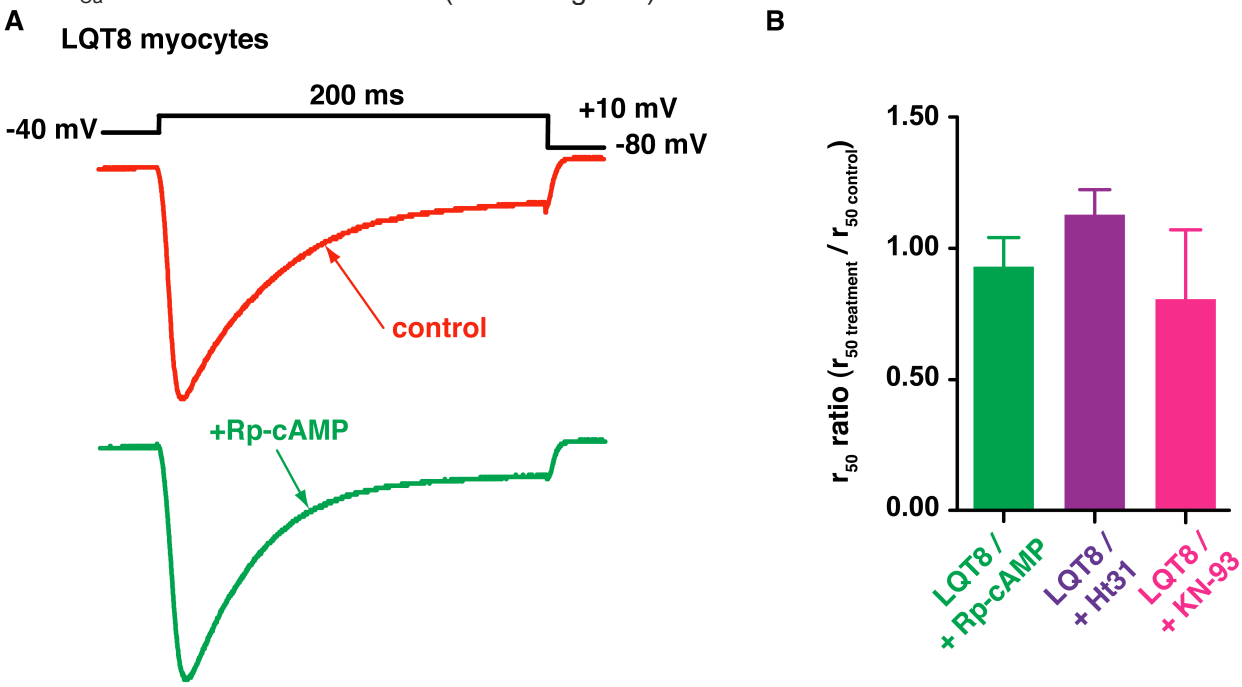

Online Figure I: CaMKII and PKA do not modulate the rate of inactivation of I_{Ca} in LQT8 myocytes. **(A)** Representative normalized I_{Ca} records from a LQT8 ventricular myocyte before and after the application of Rp-cAMP. I_{Ca} was activated by a 200 ms depolarization to +10 mV from -80 mV. **(B)** Bar plot of the fraction of I_{Ca} remaining 50 ms (r_{50}) into a depolarization pulse to +10 mV in LQT8 ventricular myocytes before and after the application of Rp-cAMP, ht31, or KN-93.

Methods and Materials

Generation of LQT8 mice

pcDNA3 plasmids encoding WT rabbit $Ca_V1.2$ Ca^{2+} channels (NCBI Reference Sequence: NC_013676.1) were provided by Dr. Diane Lipscombe. We generated the rabbit homolog of the human LQT8 (Timothy syndrome) $Ca_V1.2$ (G436R, Rabbit; G406R Human)[7]. tRFP was fused to the carboxyl terminal of $Ca_V1.2$ by fusion PCR cloning (BPS Bioscience). Then, the $Ca_V1.2$-tRFP was cut out by HindIII and cloned into the vector pBS-αMHC-hGH, a generous gift from Dr. Jeffrey Robbins (University of Cincinnati, Ohio). The construct was linearized by NotI, and the transgene was purified from vector backbone by QIAEX II Gel Extraction Kit (Qiagen). The 13kb transgene was microinjected into pronuclei of fertilized single-cell C57BL/6 × C3H mouse embyos. After injection, the eggs are surgically transferred to the oviducts of time-mated pseudopregnant foster mothers. A combination of PCR and Southern blotting of genomic DNAs identified the founders. The cardiac-specific expression of the transgene was confirmed by RT-PCR and biotinylation Western blot (Figure 1A-B).

Isolation of ventricular myocytes

Mice (WT littermates, LQT8, and LQT8/AKAP150$^{-/-}$) were euthanized with a lethal dose of sodium pentobarbital administered intraperitoneally as approved by the University of Washington Institutional Animal Care and Use Committee. Ventricular myocytes were isolated using a Langendorff perfusion apparatus as previously described [8, 9]. The isolated ventricular myocytes were kept at room temperature (22-25^{o}C) in Tyrode's solution with the following constituents (mmol/L): 140 NaCl, 5 KCl, 10 HEPES, 10 glucose, 2 $CaCl_2$, and 1 $MgCl_2$; pH 7.4 and used 0.5-6 hours after isolation.

$Ca_V1.2$ constructs and their expression in mouse embryonic fibroblasts (MEFs)

pcDNA3 plasmids encoding calcium channel accessory subunits (Ca_V-β_{2a}, GenBank accession number: M88751, and Ca_V-$\alpha_2\delta_1$, GenBank accession number: AF286488) were provided by Dr. Diane Lipscombe. Plasmids for the enhanced green fluorescent protein (EGFP) was purchased from Invitrogen. EGFP was fused to the C-terminus of $Ca_V1.2$ and $Ca_V1.2$-LQT8, yielding $Ca_V1.2$-LQT8-EGFP and $Ca_V1.2$-EGFP. Cultures of MEF cells were maintained in Dulbecco's Modified Eagle Medium supplemented with 10% fetal bovine serum, L-glutamine (2 mmol/L), 1% streptomycin and penicillin solution, 1% Modified Eagle Medium non-essential amino acids, and 100 nM 2-mercaptoethanol. Cells were transiently transfected with the pcDNA3 clones of $Ca_V1.2$-WT-EGFP or $Ca_v1.2$-LQT8-EGFP, Ca_V-β_{2a}, and Ca_V-$\alpha_2\delta_1$ using JetPEI (Polyplus). Successfully transfected cells were identified on the basis of EGFP fluorescence.

Coupled Markov chain model

Membrane currents were analyzed using a binary coupled Markov chain model originally described by Chung and Kennedy [10, 11] to simulate and fit independent records of partially coupled channels. The program was written in Matlab® language. Channel openings were identified using a half-amplitude protocol, with the quantal level for a unitary event set at 0.50 pA for currents. The activity of $Ca_v1.2$ channels during a patch-membrane recorded I_{Ca} time course was modeled as a first order, discrete Markov chain, and the Markovian transition matrix was estimated from the current and their corresponding channel opening time courses using the built-in Hidden Markov parameter estimation function in Matlab®. The estimated transition matrix was modeled as a partially coupled Markov chain where a dimensionless parameter (κ) is the coupling coefficient between fully uncoupled and fully coupled cases. In addition to the

coupling coefficient (κ), the model has two additional parameters: the channel open-to-open probability (ρ) and the channel closed-to-closed probability (ς), and together they fully describe the contribution from the fully uncoupled case to the transition matrix. For each record, the optimum set of parameters (κ, ρ, ς) for the partially coupled Markov chain model was fitted using a gradient descent algorithm.

The utility of this model is that it is a "lumped" model, where the channels switch between the binary observable states of either "open" or "closed," and therefore, instead of trying to deduce the gating kinetics of multiple channels, which involves many free parameters, our model has only three free parameters, including the coupling coefficient (κ). It does not completely describe the actual kinetics of the channel and consequently the transition probabilities obtained from this lumped model are not interpreted as rate constants.

Electrophysiology

All electrophysiological recordings were performed while cells were superfused with saline solutions at room temperature (≈ 22 ˚C). For whole-cell L-type Ca^{2+} currents (I_{Ca}), membrane potential was controlled via the patch-clamp technique using an EPC10 (HEKA) or an Axopatch 200B amplifier (Molecular Devices). Data were acquired at 10 kHz and low-pass filtered at 5 kHz. Ventricular myocytes and MEFs were continuously superfused with Tyrode's solution. Once whole-cell configuration has been successfully established in myocytes, a solution with the following constituents (mmol/L) was exchanged: 140 NMDG, 5 $CsCl_2$, 2 $CaCl_2$, 1 $MgCl_2$, 10 glucose, 10 HEPES, adjusted to pH 7.4 with HCl, and 50 μM of tetracaine was added to block SR Ca^{2+} induced Ca^{2+} release. For MEFs experiments, this solution was exchanged for a solution containing a similar composition except that $CaCl_2$ was 20 mmol/L, NMDG concentration was 120 nM, and no tetracaine was added. Pipettes for whole-cell patch-clamp were pulled using a Flaming-Brown type puller (Sutter Instruments) with nominal resistance of 1-2 MΩ and filled with a solution composed of (mmol/L): 87 Cs-aspartate, 20 CsCl, 1 $MgCl_2$, 5 MgATP, 10 EGTA, 10 HEPES, and 4.7 $CaCl_2$, adjusted to pH 7.2 with CsOH. The free [Ca^{2+}] was 150 nM, as calculated using the MaxChelator program [12]. I_{Ca} was evoked from both myocytes and MEFs by 200 ms long depolarization pulses from -80 mV to -40 to +50 mV. For myocytes, an additional 100 ms long voltage step to -40 mV immediately preceded the depolarization pulses as to inactivate Ca^{2+} conductance through voltage-gated Na^{+} channels. For experiments involving treatments with the chemical inhibitors Rp-cAMP, Ht31, and KN-93, the inhibitors were dissolved in the appropriate external solution for whole-cell I_{Ca} recordings to the appropriate concentration (100 μM for Rp-cAMP, 10 μM Ht31, and 5 μM for KN-93). We recorded post-treatment I_{Ca} 10 minutes after starting superfusion with the inhibitor solution.

For action potential (AP) recordings in ventricular myocytes, we used the whole-cell current clamp mode of the Axopatch 200B amplifier. Cells were continuously superfused with Tyrode's solution. Pipettes for AP recordings had nominal resistance of 1-2 MΩ and filled with a solution composed of (mmol/L): 30 KCl, 110 K-aspartate, 10 HEPES, 10 NaCl, 5 MgATP, adjusted to pH 7.2 with KOH. APs were excited by 5 ms long current injections of 7 nA occurring every 1 s. This relatively slow stimulation rate and low solution temperature (≈ 22 ˚C) likely prolonged the action potential of ventricular myocytes. Membrane voltage records were sampled at 10 kHz and low-pass filtered at 2 kHz. Early afterdepolarizations (EADs) were visually identified as spontaneous depolarizations in membrane voltage during phases II and III of the cardiac AP, while delayed afterdepolarizations (DADs) were visually identified as spontaneous depolarizations in membrane voltage during phase IV of the cardiac AP

We also recorded L-type Ca^{2+} channel currents from cell-attached patches in ventricular myocytes. Data were acquired using an Axopatch 200B amplifier at 10 kHz and low-pass filtered at 2 kHz. The patch pipettes were pulled using a Flaming-Brown type puller and heat polished using a microforge (Narishige) with a nominal resistance of 2-3 MΩ. The pipette solution contained (mmol/L): 20 $CaCl_2$ (charge carrier), 130 TEA, and 10^{-3} tetrodotoxin (TTX), adjusted to pH = 7.2 with HCl. Voltage gated Na^+ channels were blocked with TTX, while voltage gated K^+ channels were blocked with TEA. The L-type Ca^{2+} channel agonist BayK-8644 (500 nM) was included in the pipette solution to increase the mean open time and P_o of these channels. Currents were recorded while cells were exposed to a solution containing (mmol/L): 145 KCl, 10 HEPES, and 10 NaCl (pH = 7.4). L-type Ca^{2+} channel currents were evoked by a 1 s step depolarization to -30 mV from the holding potential of -80 mV. Membrane currents were analyzed using pCLAMP 10 (Molecular Devices). All experiments were performed at room temperature (22-25^{o}C).

Confocal imaging of Ca^{2+} signals

Ventricular myocytes were loaded with the membrane-permeable acetoxymethyl-ester form of Fluo-4 (Fluo-4 AM, Invitrogen) for measurement of $[Ca^{2+}]_i$ as previously described [13]. Cells were placed in a perfusion chamber and incubated with normal Tyrode at 22 –25 °C. Field stimulation was performed with two platinum wires (0.5 cm separation) placed at the bottom of the perfusion chamber. An IonOptix Myopacer (IonOptix Corp) stimulator was used to deliver square voltage pulses (4 ms duration) with amplitude of 35 volts at a frequency of 1 Hz. We imaged temporal fluorescence fluctuations caused by $[Ca^{2+}]$ transients using the line-scan mode (2 ms/line) of our Olympus Fluo View 1000 confocal microscope with an Olympus APON (60X, NA = 1.49) oil-immersion lens. Fluo-4 was excited with a 473 nm solid-state laser. Line-scan images were analyzed using ImageJ. Background subtracted fluorescence signals were normalized by dividing fluorescence at each point (F) with the baseline fluorescence (F_0). Spontaneous Ca^{2+} release (SCR) events were identified manually as increases in fluorescence that were not elicited by stimulation.

Analysis of the spatial distribution of $Ca_V1.2$-WT and tRFP-tagged $Ca_V1.2$-LQT8 channels

We used immunofluorescence approaches to determine the spatial distribution of $Ca_V1.2$-WT in WT and AKAP150$^{-/-}$ myocytes. To do this, myocytes were plated on BD Cell-Tak coated cover slips. Cells were allowed to attach for 4 hrs. Cells were then fixed in a solution containing 2% paraformaldehyde, 75 mM Lysine and 10 mM sodium periodate in phosphate buffer[14]. Cells were washed three times in PBS, and permeabilized with 0.075% Triton X-100/PBS and incubated for 30 min. in blocking buffer containing 2% donkey serum, 20% goat serum, and 1% bovine serum albumin in pearmeabilization solution. Specific L-type $Ca_V1.2$ channel α-1C subunit (Sigma) antibody was used for immunolabeling of L-type $Ca_V1.2$ channels. Cells were extensively washed in PBS and incubated for 2 hours with donkey anti-rabbit Alexa Fluor 488-conjugated (5 mg/ml) antibody (Molecular Probes). Cells were visualized using an Olympus Fluo View 1000 confocal laser-scanning microscope equipped with an UPLSAPO 60X water lens (NA = 1.2) and a zoom of 1.9 (pixel size = 0.19 µm).

The same confocal microscope was used to image tRFP-tagged CaV1.2-LQT8 in living, freshly dissociated LQT8 and LQT8/AKAP150$^{-/-}$ myocytes. tRFP was excited with a 559 nm laser. To quantify the number of tRFP-tagged $Ca_V1.2$-LQT8 clusters in ventricular myocytes, maximum intensity projections were generated from Z-stacks. Clusters were counted and measured using ImageJ software (NIH). In brief, projected images were loaded into ImageJ. A threshold range that enabled segmentation of clusters from the background was set and the image was

converted to a binary form. The number of clusters and their feret diameter was then obtained. For an example of this analysis see Online Figure II below.

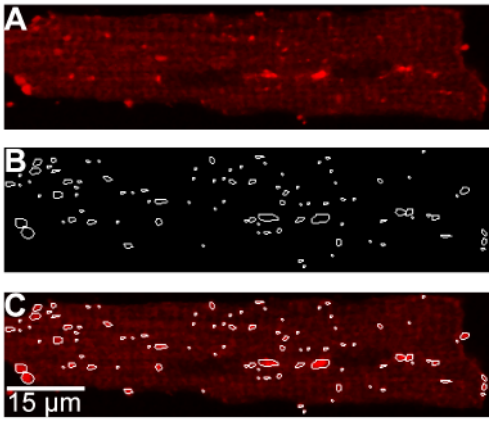

Online Figure II: Quantification of $Ca_v1.2$-LQT8 channel clusters in LQT8 myocytes. (A) A typical confocal image of a $Ca_v1.2$-LQT8 cardiomyocyte. **(B)** Outlines of clusters obtained using the particle analysis tool in ImageJ. **(C)** Confocal image shown in **(A)** with an overlay of the outlined clusters shown in **(B)**.

ECG Telemetry

Ambulatory telemetry recordings were performed in WT littermate, LQT8, AKAP150$^{-/-}$, and LQT8/AKAP150$^{-/-}$ mice. Radiotelemetry ECG monitors (DSI) were implanted intraperiotoneally, with the electrode leads sutured in place subcutaneously over the chest wall and assuming a lead II configuration. The mice were under isoflurane anesthesia during surgery, and they were given buprenorphine for analgesia for 24 hours post-surgery. A week after the surgery the mice were acclimatized to the treadmill exercise regimen. The exercise treadmill (Columbus Instruments) was started at 5 m/min and the shock grid turned on, and the speed was increased by 1 m/min every minute. The mice were exercised for 15 min per session or until they reached exhaustion, which was defined as greater than 5 s spent resting on the shock grid, at which time the shock grid was turned off. After acclimatization, the mice were exercised according to the regimen, during which their ECGs were recorded. The ECG records were analyzed using the ECG Analysis software (DSI), which automatically detected the QT intervals and arrhythmic events.

Western blots

For these experiments, we used acutely dissociated ventricular myocytes from WT littermates, LQT8, AKAP150$^{-/-}$, and LQT8/AKAP150$^{-/-}$ mice. Western blots were performed as recently described [15]. Briefly, myocytes were washed 3 times with ice-cold PBS and subsequently incubated with PBS containing 1.0 mg/ml EZ-Link Sulfo-NHS-LC-LC-biotin (Thermo Scientific) for 60 min at 4°C. After labeling, the cells were washed 3 times in ice-cold PBS containing 100 mmol/L glycine to quench and remove excess biotin reagent and by-products. Biotinylated myocytes were homogenized in RIPA buffer and cellular debris removed by centrifugation. Total protein was then determined by BCA analysis. 480 µg proteins were mixed with 120µl NeutrAvidin agarose resin (Thermo Scientific) and incubated overnight for avidin pull-down of biotinylated surface proteins. Following pull down, the supernatant comprised the non-biotinylated (cytosolic) protein fraction, while surface proteins remained bound to the avidin beads. Proteins were eluted from beads by boiling in SDS-PAGE sample buffer and analyzed

by Western blotting using standard techniques. We also performed Western blotting on crude cell homogenates, proteins pulled down by avidin, and the leftover supernatant against GAPDH, a cytosolic protein, as quality control to ensure the specificity of the biotinylation reaction against membrane proteins (Online Figure III). Anti-$Ca_V1.2$ antibody was purchased from Alomone Labs (Cat# ACC-003). Anti-GAPDH antibody was purchased from Sigma-Aldrich (Cat# G8795).

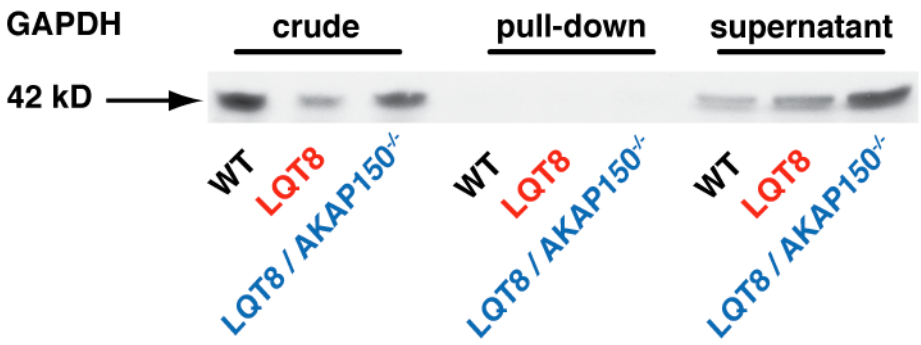

Online Figure III: Avidin pull-down of biotinylated protein is specific for sarcolemmal proteins. A Western blot showing GAPDH from crude cell homogenate (crude), proteins pulled down by avidin (pull-down), and the remaining supernatant from WT, LQT8, and LQT8/AKAP150$^{-/-}$ ventricular myocytes. GAPDH, a cytosolic protein, is absent from the avidin bound proteins.

Statistics

Data are presented as mean ± SEM. Two-sample comparisons were made using a student's T-test. A *p* value of less than 0.05 was considered significant. The asterisk (*) symbol is used in the figures to illustrate a significant difference between groups ($p<0.05$).

Supplemental references

1. Rubart M, Patlak JB, Nelson MT. Ca^{2+} currents in cerebral artery smooth muscle cells of rat at physiological Ca^{2+} concentrations. *J Gen Physiol.* 1996;107:459-472.
2. Barrett CF, Tsien RW. The Timothy syndrome mutation differentially affects voltage- and calcium-dependent inactivation of CaV1.2 L-type calcium channels. *Proc Natl Acad Sci U S A.* 2008;105:2157-2162.
3. Josephson IR, Guia A, Sobie EA, Lederer WJ, Lakatta EG, Stern MD. Physiologic gating properties of unitary cardiac L-type Ca2+ channels. *Biochemical and biophysical research communications.* 2010;396:763-766.
4. Van Haastert PJ, Van Driel R, Jastorff B, Baraniak J, Stec WJ, De Wit RJ. Competitive cAMP antagonists for cAMP-receptor proteins. *The Journal of biological chemistry.* 1984;259:10020-10024.
5. Vijayaraghavan S, Goueli SA, Davey MP, Carr DW. Protein kinase A-anchoring inhibitor peptides arrest mammalian sperm motility. *The Journal of biological chemistry.* 1997;272:4747-4752.
6. Sumi M, Kiuchi K, Ishikawa T, Ishii A, Hagiwara M, Nagatsu T, Hidaka H. The newly synthesized selective Ca2+/calmodulin dependent protein kinase II inhibitor KN-93 reduces dopamine contents in PC12h cells. *Biochemical and biophysical research communications.* 1991;181:968-975.

7. Erxleben C, Liao Y, Gentile S, Chin D, Gomez-Alegria C, Mori Y, Birnbaumer L, Armstrong DL. Cyclosporin and Timothy syndrome increase mode 2 gating of CaV1.2 calcium channels through aberrant phosphorylation of S6 helices. *Proc Natl Acad Sci U S A.* 2006;103:3932-3937.

8. Rossow CF, Dilly KW, Santana LF. Differential Calcineurin/NFATc3 Activity Contributes to the I_{to} Transmural Gradient in the Mouse Heart. *Circ Res.* 2006;98:1306-1313.

9. Shioya T. A simple technique for isolating healthy heart cells from mouse models. *J Physiol Sci.* 2007;57:327-335.

10. Chung SH, Kennedy RA. Coupled Markov chain model: characterization of membrane channel currents with multiple conductance sublevels as partially coupled elementary pores. *Math Biosci.* 1996;133:111-137.

11. Navedo MF, Cheng EP, Yuan C, Votaw S, Molkentin JD, Scott JD, Santana LF. Increased coupled gating of L-type Ca^{2+} channels during hypertension and Timothy syndrome. *Circ Res.* 2010;106:748-756.

12. Patton C, Thompson S, Epel D. Some precautions in using chelators to buffer metals in biological solutions. *Cell Calcium.* 2004;35:427-431.

13. Nichols CB, Rossow CF, Navedo MF, Westenbroek RE, Catterall WA, Santana LF, McKnight GS. Sympathetic Stimulation of Adult Cardiomyocytes Requires Association of AKAP5 With a Subpopulation of L-Type Calcium Channels. *Circ Res.* 2010;107:747-756.

14. McLean IW, Nakane PK. *J Histochem Cytochem* 1974; 22:1077-1083.

15. Bannister JP, Adebiyi A, Zhao G, Narayanan D, Thomas CM, Feng JY, Jaggar JH. Smooth muscle cell alpha2delta-1 subunits are essential for vasoregulation by CaV1.2 channels. *Circulation research.* 2009;105:948-955.